

Supplemental information

Novel AAV variants with improved tropism for human Schwann cells

Matthieu Drouyer, Tak-Ho Chu, Elodie Labit, Florencia Haase, Renina Gale Navarro, Deborah Nazareth, Nicole Rosin, Jessica Merjane, Suzanne Scott, Marti Cabanes-Creus, Adrian Westhaus, Erhua Zhu, Rajiv Midha, Ian E. Alexander, Jeff Biernaskie, Samantha L. Ginn, and Leszek Lisowski

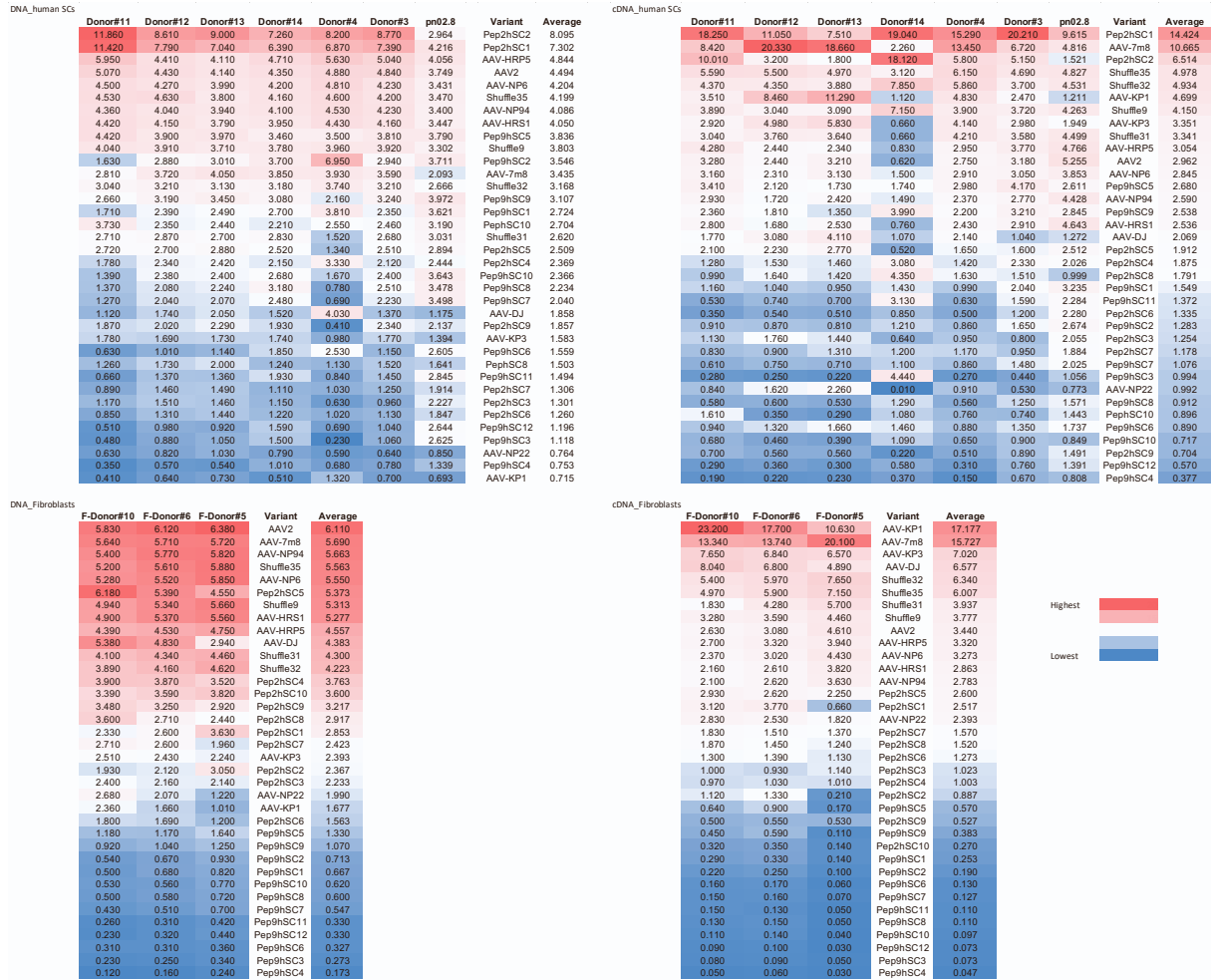


Figure S2. Performance of selected AAV variants in primary hSCs and in fibroblasts. Heat maps show the performance of selected variants. Percentage of NGS reads mapped to each AAV capsid (average of n = 2 barcodes/capsid) in seven primary SCs cultures and in three fibroblast cultures at both the level of DNA (cell entry, physical transduction) and mRNA (expression, functional transduction). Data is normalized to the ‘pre-mix pool’.

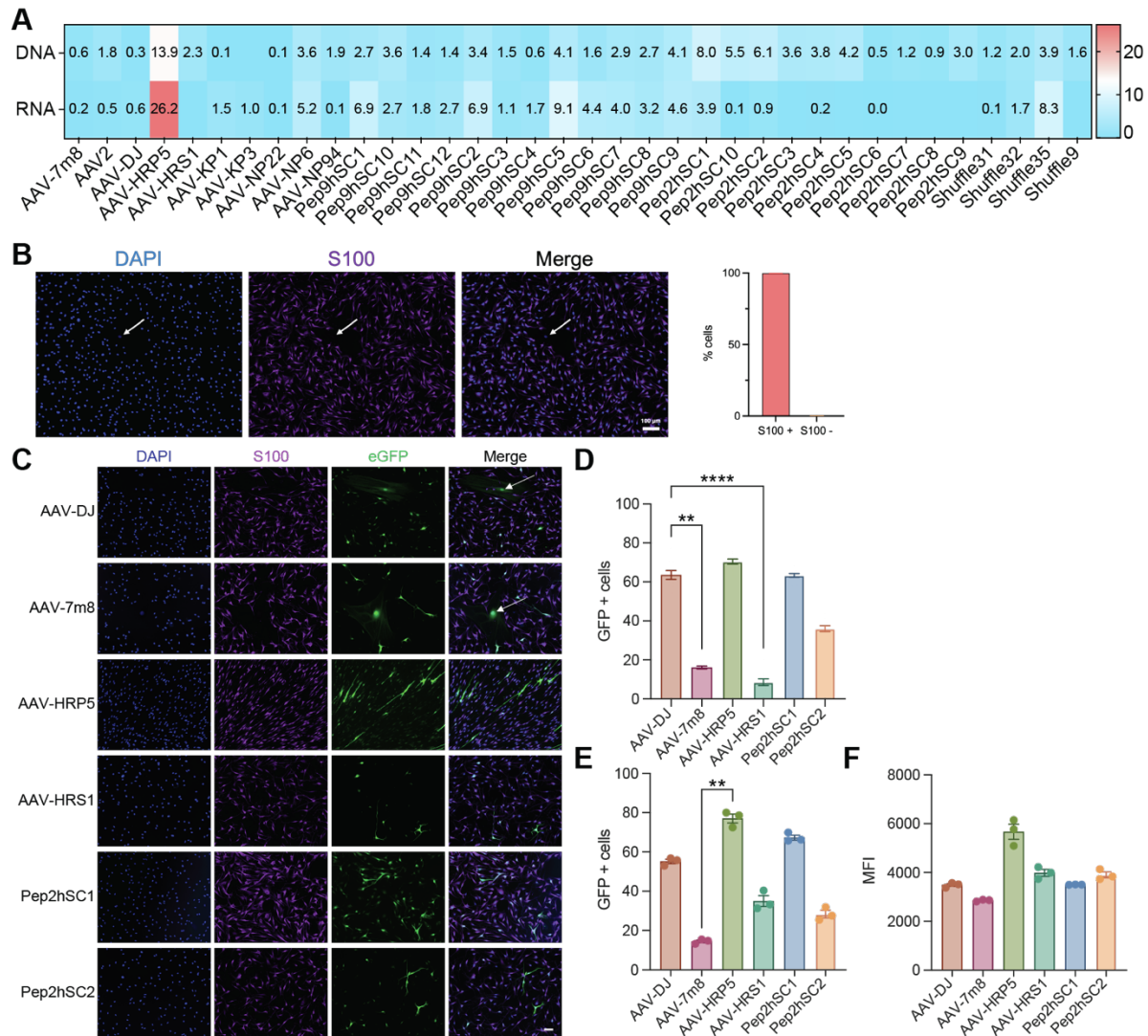


Figure S3. Assessment of AAV transduction on rat SCs.

(A) Analysis of barcoded variants with capsid recovery achieved at the level of both cell entry (DNA) and transgene expression (mRNA). Heat-map indicates the performance of each capsid as a percentage of total NGS reads for each cell type. Values are normalized to 'pre-mix pool' and are the average of 2 barcodes. (B and C) Rat SCs were transduced with the indicated variants (1,000 vg/cell) and analyzed by flow cytometry. (D) Characterization of the primary rat SC cultures derived from rat nerve segment. Representative images of rat and SC cultures stained with DAPI (blue) and the SCs marker S100 (purple). Quantification of the S100+ and S100- cells in three independent cultures. (E) Representative images of pure cultured rat SCs transduced with eGFP reporter AAVs packaged using indicated capsids (1,000 vg/cell). Blue: DAPI, purple: S100 (SCs marker), green: AAV-encoded GFP. Scale bar: 50 μ m. (F) Percentage of eGFP+/S100+ cells. Quantification was performed from ≥ 10 images per variants with ≥ 80 cells counted per image. P values were determined by one-way ANOVA non-parametric Kruskal-Wallis test with Dunn's multiple comparison test (** $p \leq 0.01$; **** $p \leq 0.0001$). Data is represented as mean \pm SEM.

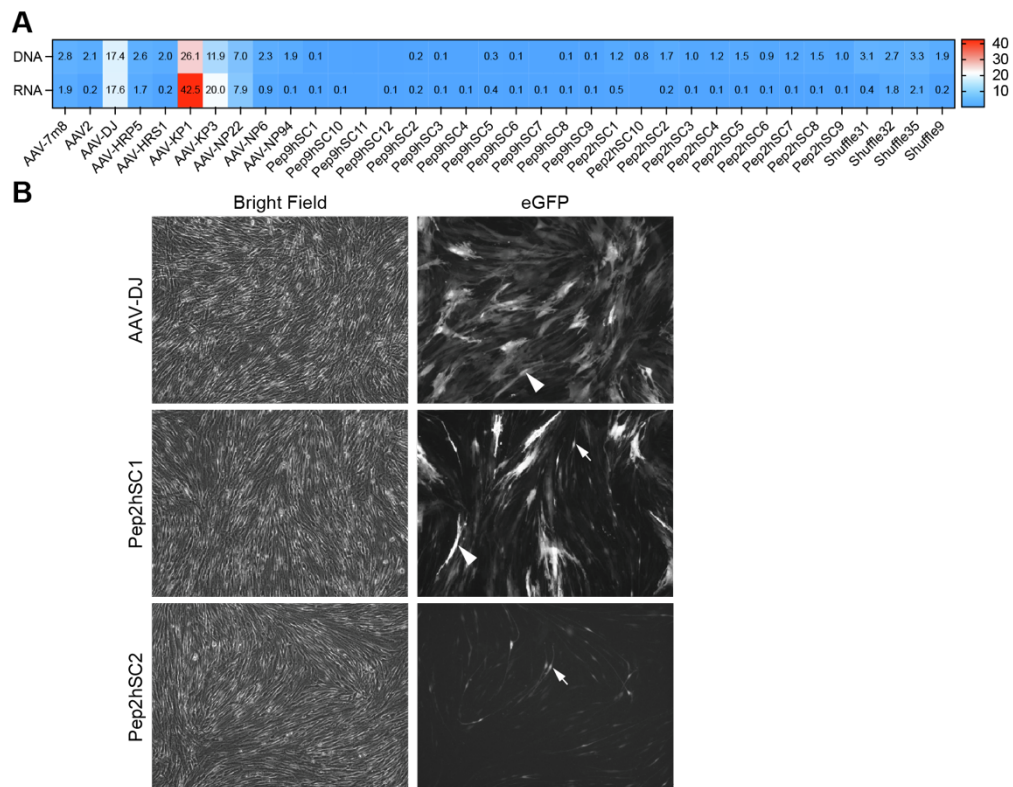


Figure S4. Assessment of AAV transduction on mouse SCs.

(A) Analysis of barcoded variants with capsid recovery achieved at the level of both cell entry (DNA) and transgene expression (mRNA). Heat-map indicates the performance of each capsid as a percentage of total NGS reads for each cell type. Values were normalized to 'pre-mix pool' and are the average of 2 barcodes. (B) Bright-field and fluorescence images 48 hours after AAV-GFP transduction of mouse SCs. Examples of transduced fibroblasts (arrowheads) and mouse SCs (arrows) are shown.

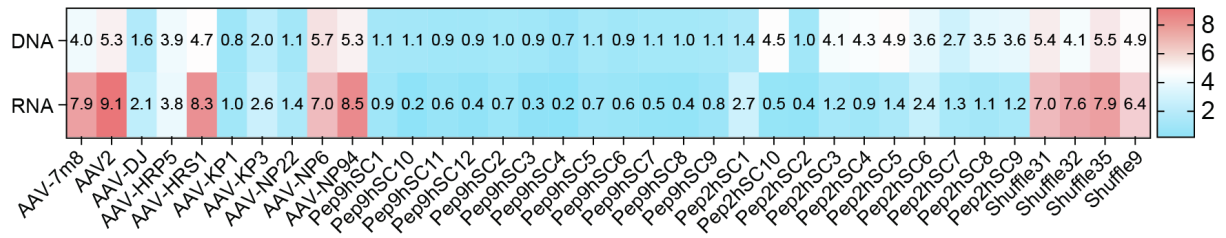


Figure S5. Assessment of AAV transduction on immortalized hSCs.

Analysis of barcoded variants with capsid recovery achieved at the level of both cell entry (DNA) and transgene expression (mRNA). Heat-map indicates the performance of each capsid as a percentage of total NGS reads from two transductions. Values were normalized to the 'pre-mix pool' and are the average of 2 barcodes.

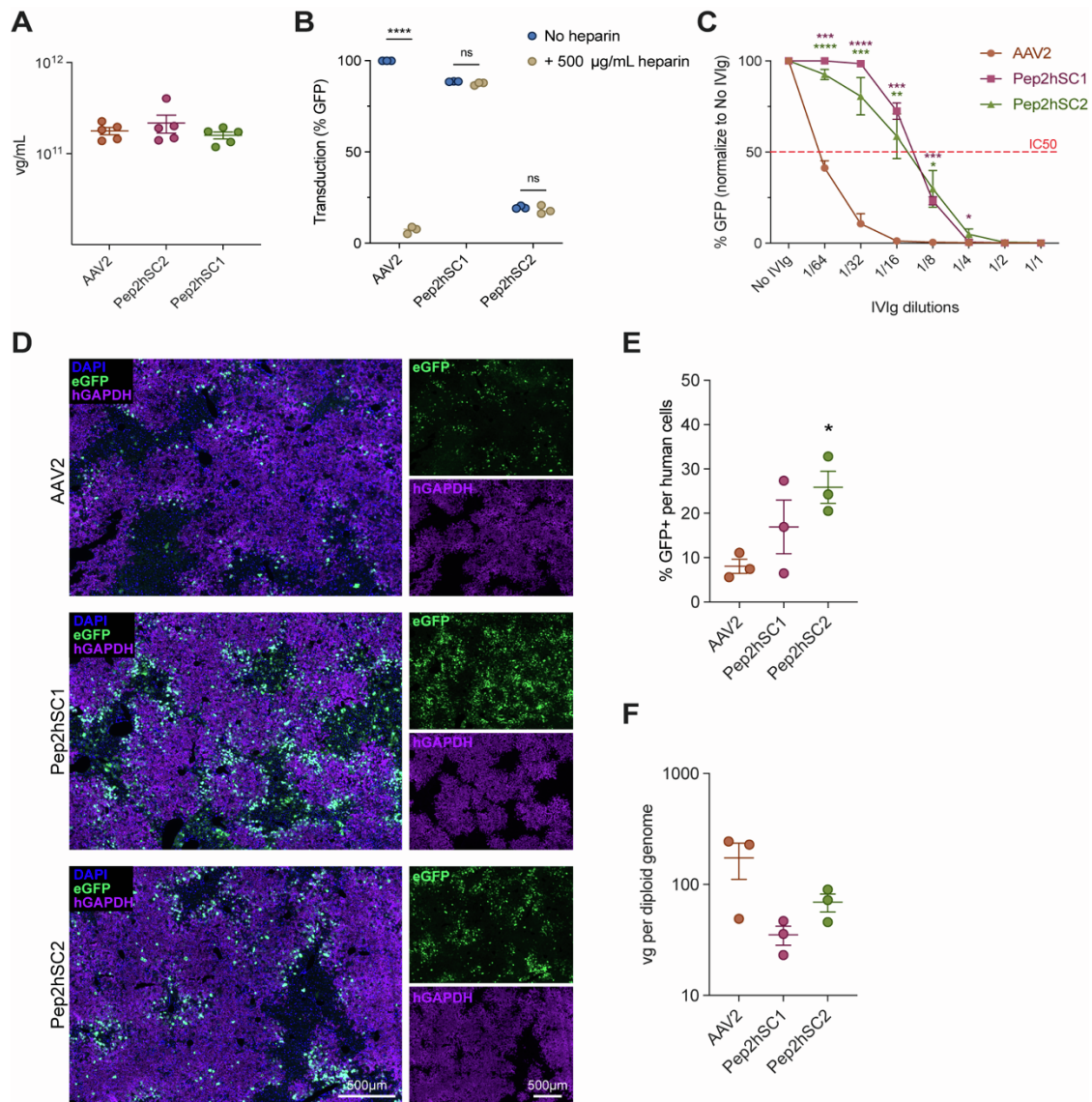


Figure S6. Characterisation of novel AAV capsid variants.

(A) Comparison of recombinant AAV crude production. Data are presented as mean \pm SEM ($n = 5$ independent single dish lysate). (B) Heparin competition assay. AAV vector variants and the parental AAV2 were pre-incubated with heparin or not. Transduction efficiency on HEK293T cells was quantified by FACS according to eGFP positive cells 72h after transduction ($n = 3$ independent experiments). Data are represented as means \pm SEM. Statistical significance was calculated using the two-tailed Mann-Whitney test by comparing vector performance with and without the presence of soluble heparin (**** $p \leq 0.0001$; n.s., $p > 0.05$). (C) Neutralization assay of indicated AAV vectors following pre-incubation with human IVIg prior to transduction of HEK293T cells. The percentage of eGFP-positive cells 72h after transduction was analyzed by flow cytometry ($n = 4$ independent experiments). The dotted red line represents IVIg-mediated inhibition of AAV transduction by 50%. P values were determined by ordinary two-way ANOVA using Šidák's multiple comparison test (* $p \leq 0.05$; ** $p \leq 0.01$, *** $p \leq 0.001$; **** $p \leq 0.0001$). Data is shown as mean \pm SEM. (D-F) Evaluation of novel AAV variants in the humanized FRG (hFRG) model. (D) Representative images of hFRG mice liver tissue following I.V. injection with either AAV-DJ, Pep2hSC1 or Pep2hSC2 (dose = 2×10^{11} vg; $n = 3$ per variant). Human hepatocytes (purple), vector-expressed eGFP (green), DAPI (blue). Scale bar: 500µm. (E) Quantification of the percentage of transduced

human hepatocytes, individual data points represent the average of 11-15 human clusters per mouse. (F) AAV vector genomes per diploid cell in human hepatocyte cells. (F) Quantification of (D) the percentage of transduced human hepatocytes, Individual data points represent the average of 11-15 human clusters per mouse. Data are represented as mean \pm SEM.

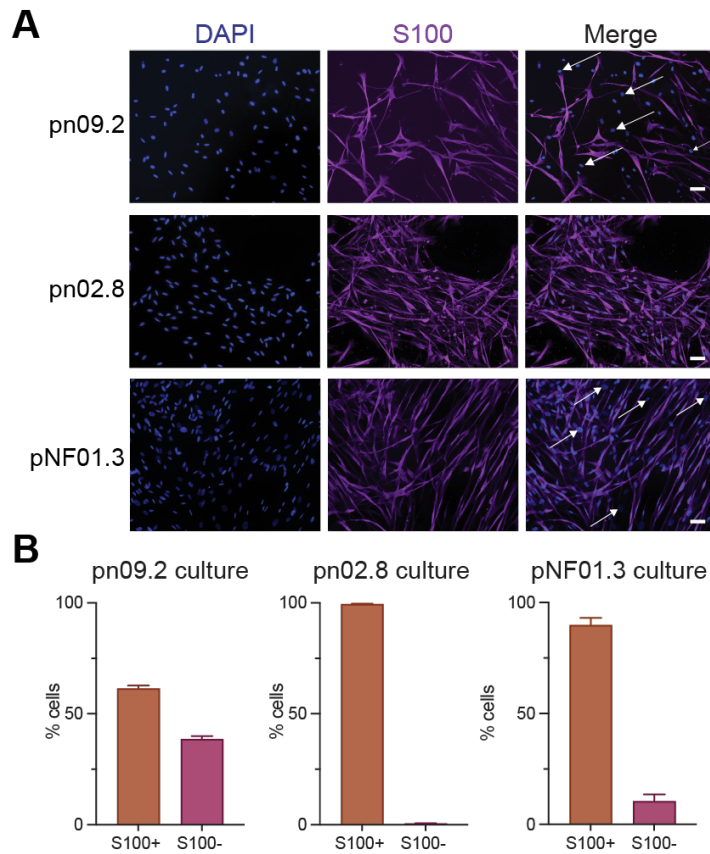


Figure S7. Characterisation of the primary human SC cultures.

(A) Representative images of human pn09.2, pn02.8 and pNF01.3 SC cultures stained with DAPI (blue) and the SCs marker S100 (purple). Arrows indicate cells that are S100-. Scale bar, 50 μ m. (B) Quantification of the S100+ and S100- cells in three independent cultures shows that pn09.2 culture contained both population with on average 60% of S100 positive and 40% of S100 negative cells, pNF03.1 culture contained both population with on average 90% of S100 positive and 10% of S100 negative cells while pn02.8 culture contained only S100 positive cells.

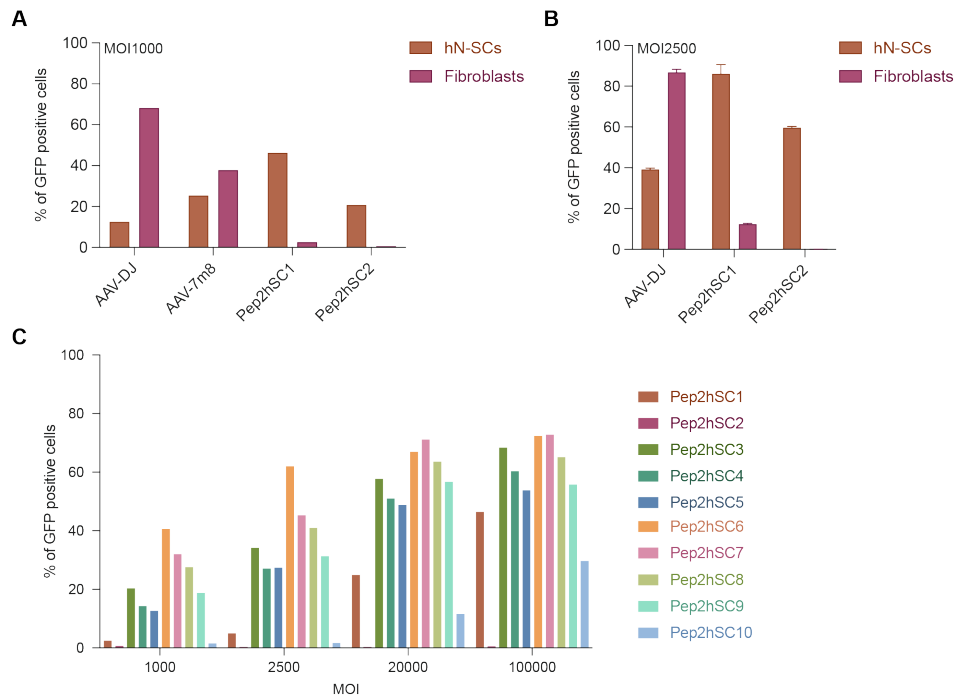


Figure S8. Transduction efficiency of selected variants for primary human SCs and fibroblasts.

(A-C) hN-SCs or fibroblast cells were transduced with vectors encoding a CMV-eGFP transgene at the doses indicated. 3 days post transduction cells were analysed by flow cytometry according to eGFP expression.

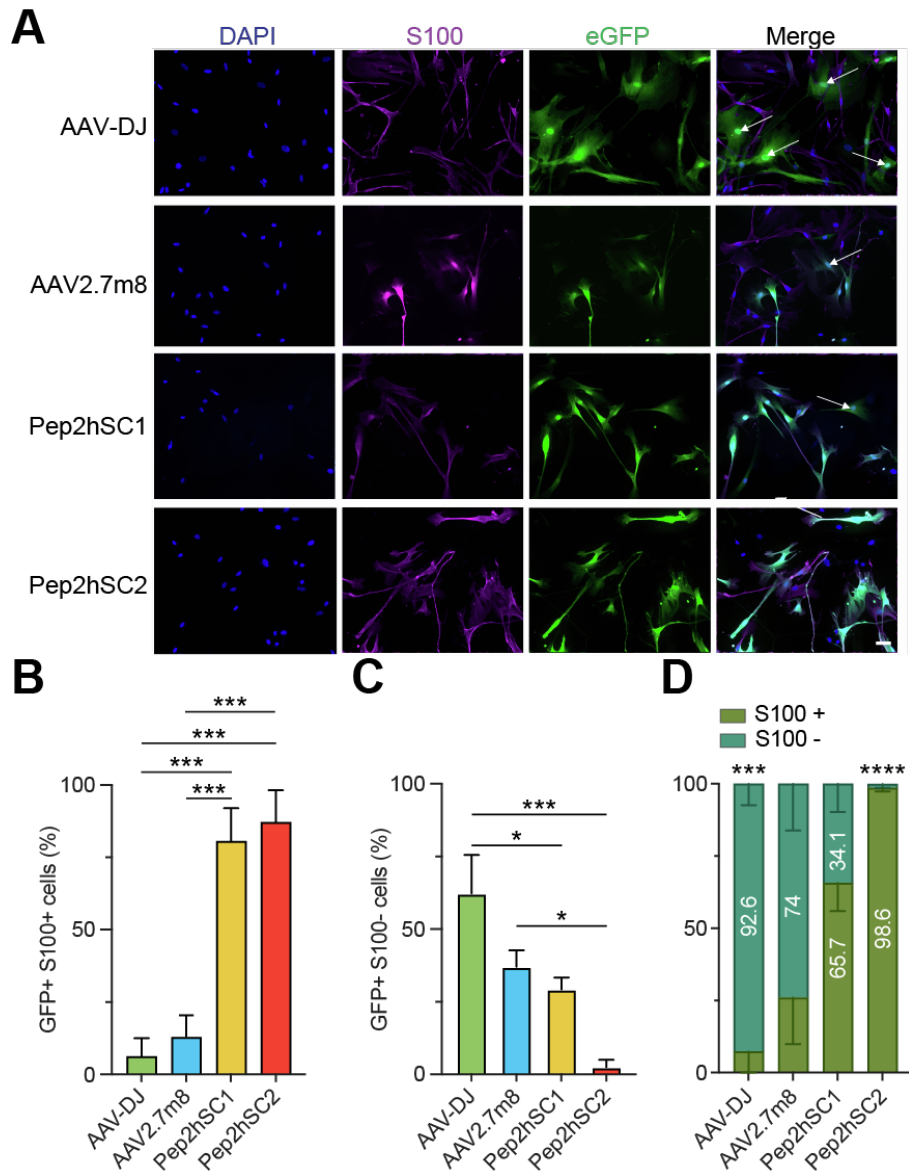


Figure S9. Transduction of pn09.2 SC culture with top AAV variants at MOT 10,000.

(A) Representative immunofluorescence images of mixed cultured hSCs transduced with indicated AAV variants encoding an eGFP reporter (10,000 vg/cell). Arrows indicate eGFP+/S100- cells. Scale bar, 50 μ m. (B and C) Percentage of (B) eGFP+/S100+ cells, (C) eGFP+/S100- cells. Quantification was performed using ≥ 30 cells per image, and ≥ 4 images per variant. P values were determined by one-way ANOVA with Holm-Sidak's multiple comparison test (* $p \leq 0.05$; *** $p \leq 0.001$). Data are given as mean \pm SEM. (D) Proportion of eGFP+ cells in the mixed hSC culture. Percentages of S100+ and S100- cells among total eGFP+ cells were calculated. P values were determined by unpaired t-test (*** $p \leq 0.001$; **** $p \leq 0.0001$).

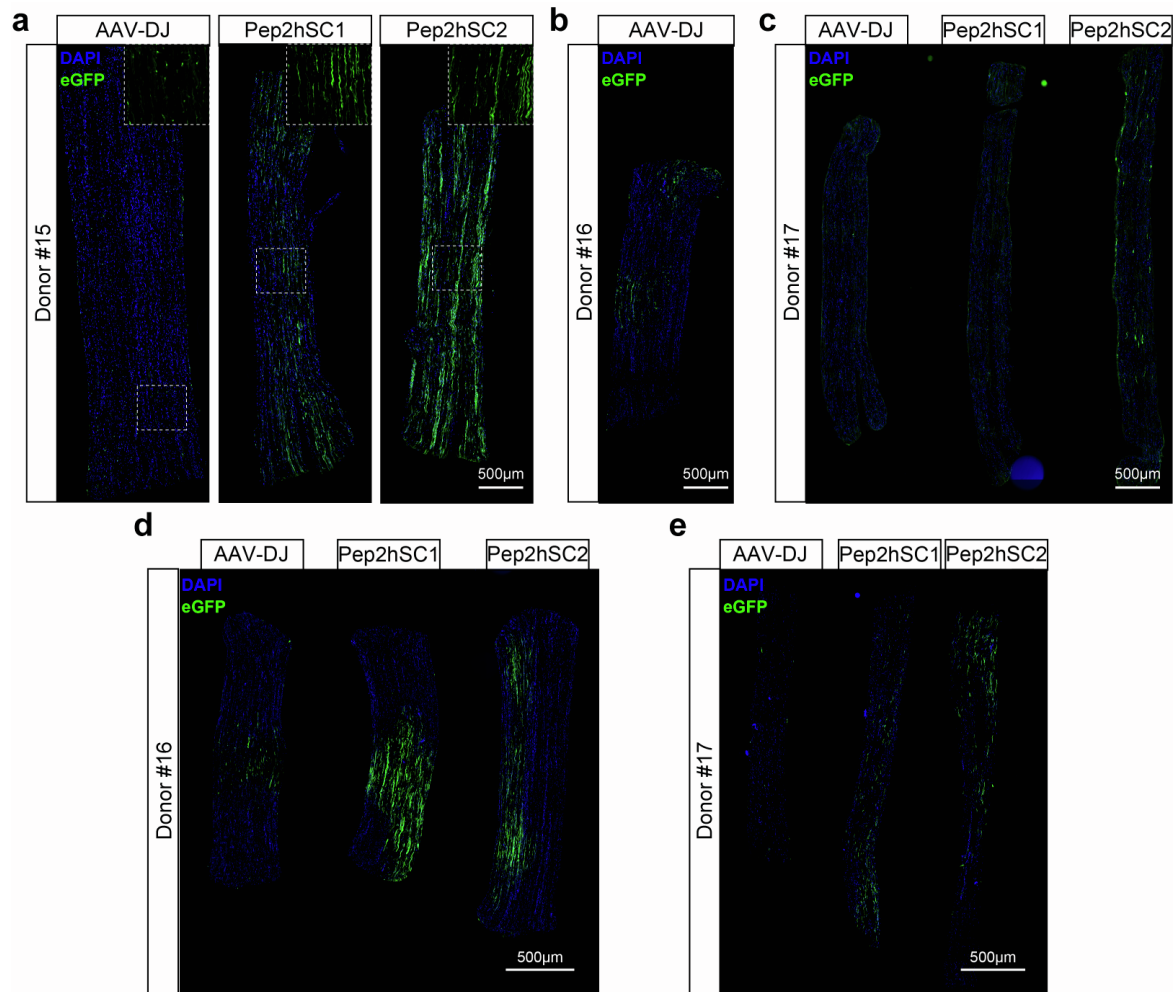


Figure S10. eGFP expression in human nerve segments.

Immunofluorescence of longitudinal sections of human sural nerve segments at (A-C) 7 days post injection and (D and E) 14 days post injection. Nerve segments (0.5cm) were injected with AAV-DJ, Pep2hSC1 or Pep2hSC2 vectors encoding a CMV-eGFP transgene (1×10^{10} vg dose per segment). DAPI (blue), AAV-encoded eGFP (green). Scale bar: 500μm.

Donor#15: 42-year-old male; Donor#16: 44-year-old male, Caucasian; Donor#17: 73-year-old male, Asian.

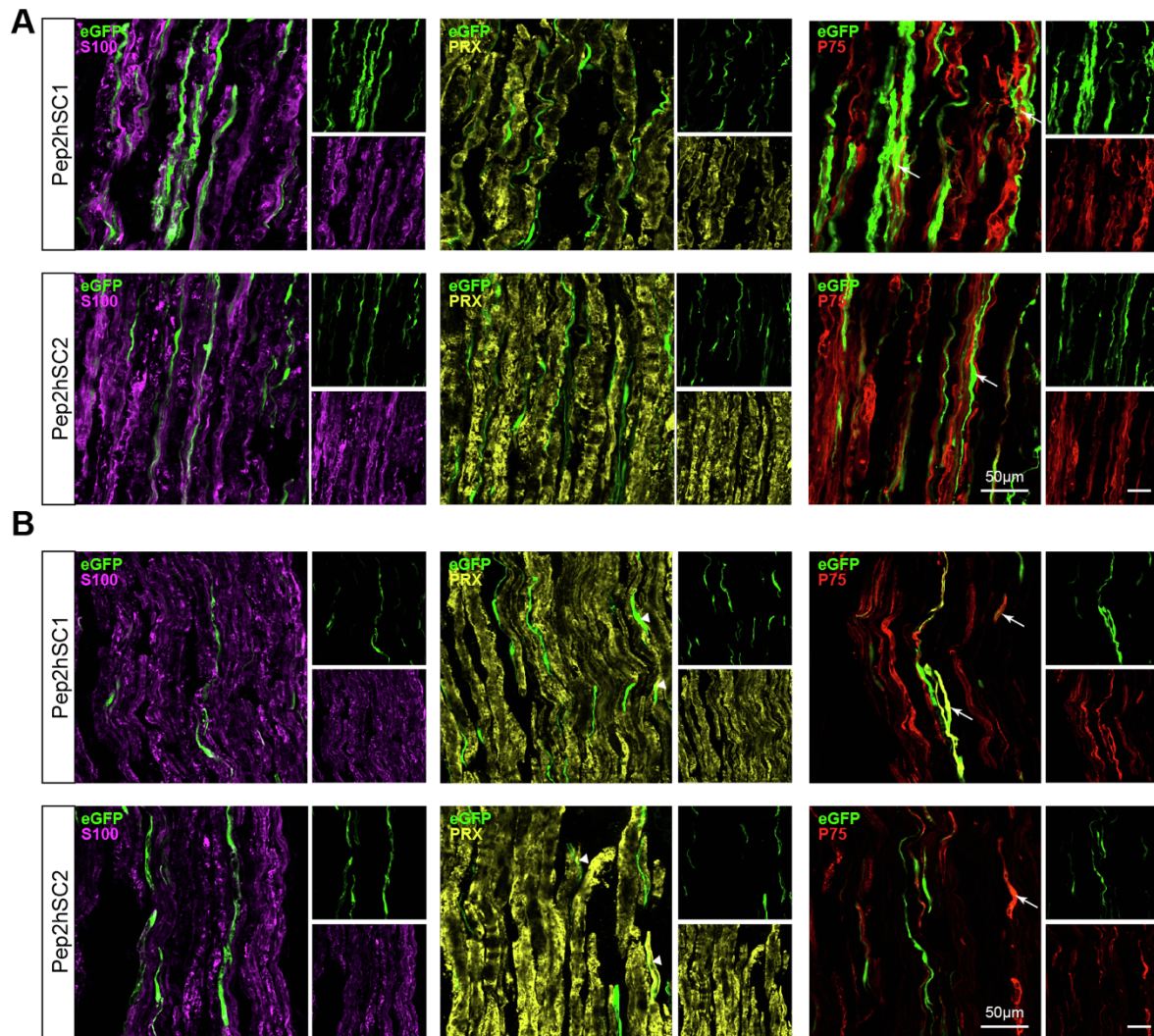


Figure S11. Immunolabeling for myelinating and non-myelinating SCs.

(A and B) Confocal microscopy images showing double immunostaining for eGFP and various markers on longitudinal sections (A) for Donor#16 and (B) for Donor#17. The sections were stained with either S100 (purple) for SCs, PRX (yellow) for myelinating SCs, or P75 (red) for non-myelinating SCs. Arrowheads in the right panel images show colocalization with non-myelinating SC marker P75. Donor#17 had some eGFP+ and PRX positive cells (arrows). Scale bar: 50µm.

Donor#16: 44-year-old male, Caucasian; Donor#17: 73-year-old male, Asian.

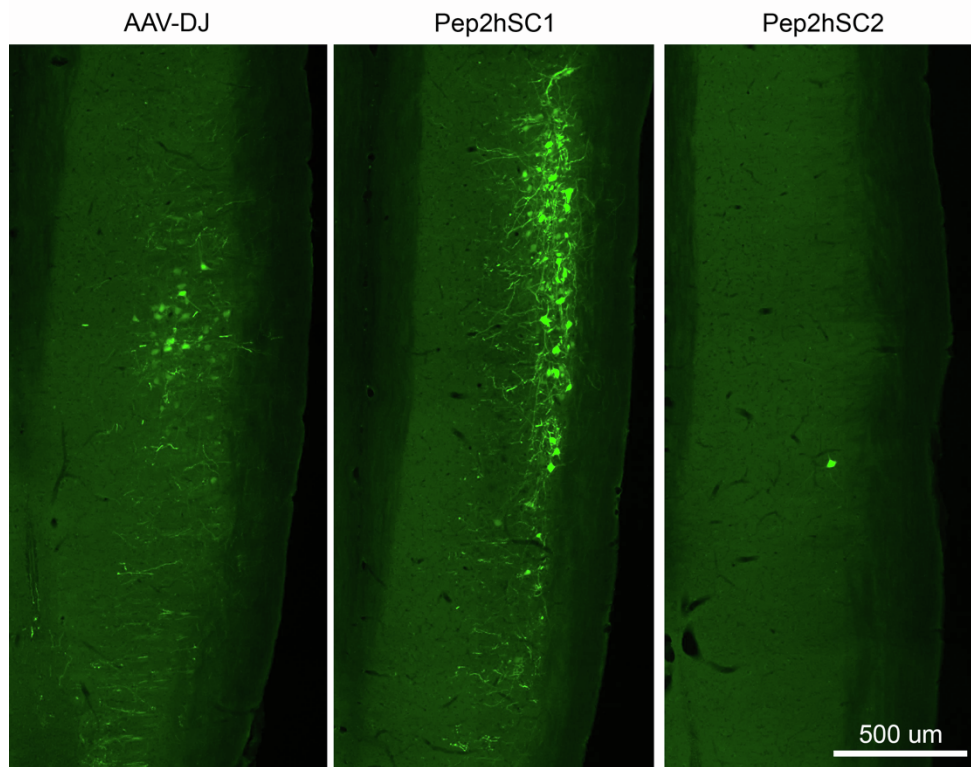


Figure S12. eGFP expression in spinal cord of mice administered by intraneural injection. Representative images of longitudinal spinal cord sections of mice following intraneural injection with either AAV-DJ, Pep2hSC1 or Pep2hSC2 (dose = 2×10^{10} vg; n = 1 per variant). Scale bar: 500 μ m.

Table S1. Information of donors used in studies conducted in primary hSC and fibroblast cultures and with *ex vivo* nerve explants.

Cell/Donor ID	Skin/Nerve/Fibroblast	Race/ethnicity	Age	Sex	Sources
pn02.8	Nerve	/	55	M	/
pNF01.3	Nerve tumor	/	/	/	Biopsy
pn09.2	Nerve	/	/	/	/
Donor#1	Nerve	Caucasian	28	M	Autopsy
Donor#2	Nerve	Asian	47	M	Autopsy
Donor#3	Nerve	Caucasian	58	M	Autopsy
Donor#4	Nerve	Caucasian	62	M	Autopsy
Donor#5	Fibroblast	Caucasian	50	F	Biopsy
Donor#6	Fibroblast	Caucasian	60	M	Biopsy
Donor#7	Skin	Caucasian	51	F	Biopsy
Donor#8	Skin	Caucasian	56	F	Biopsy
Donor#9	Fibroblast	Caucasian	63	M	Autopsy
Donor#10	Fibroblast	Caucasian	48	F	Biopsy
Donor#11	Skin	Caucasian	26	M*	Biopsy
Donor#12	Skin	Caucasian	64	F	Biopsy
Donor#13	Skin	Caucasian	49	F	Biopsy
Donor#14	Nerve	Caucasian	66	M	Autopsy
Donor#15	Nerve	/	42	M	Autopsy
Donor#16	Nerve	Caucasian	44	M	Autopsy
Donor#17	Nerve	Asian	73	M	Autopsy

Table S2. Information of primary human hepatocyte donors used to engraft FRG mice.

Sex	Internal ID	Albumin level [mg/ml]	Experiment	Cell origin	Replacement Index
Female	311	16.207	AAV2_2e11vg	Lonza #HUM181971	90.7%
Female	323	14.188	AAV2_2e11vg	Lonza #HUM181971	85.5%
Female	70	16.446	AAV2_2e11vg	Lonza #HUM181971	81.0%
Female	548	10.506	Pep2hSC1_2e11vg	Lonza #HUM181141	78.4%
Female	392	15.481	Pep2hSC1_2e11vg	Lonza #HUM181141	88.6%
Female	434	14.224	Pep2hSC1_2e11vg	Lonza #HUM181971	84.2%
Female	589	13.72	Pep2hSC2_2e11vg	Lonza #HUM181141	37.3%
Female	438	17.057	Pep2hSC2_2e11vg	Lonza #HUM181971	81.6%
Female	469	15.331	Pep2hSC2_2e11vg	Lonza #HUM181971	89.1%

